

# Supplemental Materials

*Molecular Biology of the Cell*

Santos et al.

## Supplemental Materials

### Supplemental Figure Legends

**Supplemental Figure 1. EGF-stimulated PLC $\gamma$ 1 activation and PLC $\gamma$ 1 silencing in RPE cells.** (A) RPE cells were stimulated with 5 ng/mL EGF for 0-10 min (as indicated), followed by preparation of whole cell lysates and immunoblotting to detect phospho-PLC $\gamma$ 1. Shown are representative immunoblots (left panels), as well as mean  $\pm$  SE of the phospho-PLC $\gamma$ 1 signal intensity (right panels),  $n = 3$ . (B) RPE cells were transfected with siRNA to silence PLC $\gamma$ 1 or non-targeting siRNA (control). Whole cell lysates were resolved by western blotting and probed with anti-PLC $\gamma$ 1 specific antibodies or anti-actin antibodies (loading control). Shown are representative immunoblots (left panel), as well as mean  $\pm$  SE of the PLC $\gamma$ 1 signal intensity (right panels),  $n = 3$ , \*,  $p < 0.05$ .

**Supplemental Figure 2. EGF internalization.** (A) RPE cells were treated with siRNA to silence clathrin heavy chain (clathrin), or non-targeting siRNA (control). EGF internalization was measured at 100 ng/mL of biotin-xx-EGF. Shown are the means  $\pm$  SE of 4 independent experiments. \*,  $p < 0.05$ . While EGFR may internalize by non-clathrin mechanisms under some conditions (e.g. when stimulated with high doses of EGF in some cells (Sigismund *et al.*, 2008)), these results indicate that EGF internalization is very largely clathrin-dependent in RPE cells, both at low dose of EGF (5 ng/mL, (Garay *et al.*, 2015)) and at high doses (100 ng/mL) EGF (this figure). (B) RPE cells were treated with 10  $\mu$ M BAPTA-AM (BA) for 15 min, then subjected to the measurement of cell-associated EGF (using EGF internalization assay modification that omits quenching of non-internalized, surface bound biotin-xx-EGF, see *Materials and Methods*). Perturbation of Ca<sup>2+</sup> signaling does not impact the association of EGF ligand with EGFR at 37C.

**Supplemental Figure 3. Silencing of dynamin 1 has no effect on EGF internalization and cyclosporin A effectively perturbs calcineurin in RPE cells.** (A-B) RPE cells were treated with siRNA to silence dynamin 1 (as per (Reis *et al.*, 2015)), or non-targeting siRNA (control). (A) Whole cell lysates were resolved by western blotting and probed with anti-dynamin1 specific antibodies or anti-actin antibodies (loading control). Shown are representative immunoblots (left panel), as well as mean  $\pm$  SE of the dynamin1 signal intensity (right panels),  $n = 3$ , \*,  $p < 0.05$ . (B) EGF internalization was measured (at 5 ng/mL EGF). Shown are the means  $\pm$  SE of 4 independent experiments in each condition. (C-D) NFAT undergoes calcineurin-dependent nuclear translocation in response to a gain in cytosolic calcium (Aramburu *et al.*, 1999). RPE cells were transfected with cDNA encoding GFP-NFAT, treated with 10  $\mu$ M cyclosporin A (CsA) for 30 min, then treated with 5 ng/mL EGF for 5 min, as indicated. Shown in (C) are representative GFP-NFAT and DAPI epifluorescence images obtained using a Leica DM5000 B epifluorescence microscope using a DFC350FX camera (Leica Microsystems, Wetzlar, Germany), scale = 20  $\mu$ m and in (D) the mean  $\pm$  SE of cellular nuclear/cytoplasmic GFP-NFAT fluorescence ratio.

**Supplemental Figure 4. Effective sorting of CLSs into cohorts based on EGFR and TfR content in TIRF images.** The data presented in Figure 5C was obtained by sorting CLSs into cohorts based on content of signal from rhodamine-EGF and A647-Tfn, indicating the CLS levels of EGFR and TfR, respectively. Shown are the integrated fluorescence intensities corresponding to EGF (A-B) and Tfn (C-D) within each CLS in each cohort. Shown in A and C

are the sum per cell  $\pm$  SE of the fluorescence intensities of indicated ligands, in the following CLS cohorts: (i) All CLSs, (ii) the CLSs positive for EGF and/or Tfn: (*EGFR or Tfn*)+CCPs and (iii) the CCPs negative for both EGFR and Tfn: (*EGFR or Tfn*)-CCPs. The (*EGFR or Tfn*)+CCPs cohort (indicated with an asterisk) is further sub-classified into cohorts based on the presence of one or both ligands. Also shown are EGF (**B**) and Tfn (**D**) intensities within these cohorts, as indicated. These experiments indicate the effective sorting of CLSs by content of EGF and Tfn for the approach used for the analysis presented in **Figure 5C**.

**Supplemental Figure 5. Full-size representative spinning disc confocal images of RPE GFP-CLC cells treated with rho-EGF and A647-Tfn.** As described for Figure 5D-F, RPE cells stably expressing clathrin light chain fused to eGFP (eGFP-CLCa) were treated with 20 ng/mL rhodamine-EGF (rho-EGF) and 10  $\mu$ g/mL A647-Tfn for the indicated time, followed by immediate fixation. Shown are representative fluorescence micrographs obtained by spinning disc confocal microscopy of cells treated with ligands for 5 min, corresponding to the ventral z-section, and two dorsal z-sections (middle and top of the cell). For each set of z-section series, scale 20  $\mu$ m (top row) and 5  $\mu$ m (bottom row, corresponding to enlarged images of the region shown in the merged image of the top row). These images correspond to the analysis presented in **Figure 5D-F**.

**Supplemental Figure 6. Effective sorting of CLSs into cohorts based on EGFR and Tfn content in spinning disc confocal images.** The data presented in Figure 5D-F was obtained by sorting CLSs into cohorts based on content of signal from rhodamine-EGF and A647-Tfn. Shown are the mean fluorescence intensities corresponding to EGF (top panels) and Tfn (bottom panels) within each CLS in each cohort. Shown in are median (bar) and 25th/75th percentiles (boxes) of the fluorescence intensities corresponding to each ligand, in cohorts of CLSs, as indicated: CLSs positive for EGF but negative for Tfn (“EGF only CLSs”), CLSs positive for Tfn but negative for Tfn (“Tfn only CLSs”), CLSs positive for both Tfn and EGF (“EGF and Tfn CLSs”) and CLS negative for both (“Negative for EGF and Tfn”). These experiments indicate the effective sorting of CLSs by content of EGF and Tfn for the approach used for the analysis presented in **Figure 5D-F**. The number of CLSs and cells analyzed, respectively, in each z-section and each time of ligand addition is as follows: 1 min, ventral: 60644, 42; 1 min, middle: 93878, 42; 1 min, top: 15938, 41; 3 min, ventral: 57496, 35; 3 min, middle: 72380, 35; 3 min, top: 10894, 36; 5 min, ventral: 64538, 37; 5 min, middle: 78012, 37; 5 min, top: 11528, 38; 10 min, ventral: 52981; 10 min, middle: 60737, 34; 10 min, top: 7726, 35.

**Supplemental Figure 7. Full-size representative TIRF-M images of RPE GFP-CLC cells treated with A555-EGF or A555-Tfn.** Shown in Figure 6A-B are images of RPE cells stably expressing eGFP-LCa and treated with A555-EGF or A555-Tfn for 5 min, followed by fixation and imaging with TIRF microscopy. Shown here are the full-sized images of the representative images shown in Figure 6A-B, with a white box showing the area enlarged in Figure 6A-B, scale, 20  $\mu$ m.

**Supplemental Figure 8. Dynamics of EGF+ sCLSs and CCPs.** RPE cells stably expressing clathrin light chain fused to eGFP (eGFP-CLCa) were pre-treated with 10  $\mu$ M BAPTA-AM for 15 min, and then treated with 20 ng/mL rhodamine-EGF (Rho-EGF) during time-lapse imaging by TIRF-M. Time-lapse image series were subjected to automated detection, tracking, and analysis of CCPs as described in *Materials and Methods*, allowing identification of EGF+ sCLSs and CCPs. Shown are (**A**) the mean rho-EGF fluorescence intensities within CCPs grouped into CCP

lifetime cohorts; error bars reflect cell-to-cell variation and dotted lines indicated the disappearance of clathrin from the TIRF field and **(B)** representative CCP trajectories depicting micrographs obtained by TIRF-M centered on the detected object and the quantification of the fluorescence intensity of eGFP-CLC and Rho-EGF in these structures. **(C)** Shown is a histogram depicting the frequency of EGF+ CCPs of indicated lifetimes.

**Supplemental Figure 9. Dynamics of Tfn+ CCPs.** RPE cells stably expressing clathrin light chain fused to eGFP (eGFP-CLCa) were pre-treated with 10  $\mu$ M BAPTA-AM for 15 min, and then treated with 100 ng/mL A647-Tfn during time-lapse imaging by TIRF-M. Time-lapse image series were subjected to automated detection, tracking, and analysis of CCPs as described in *Materials and Methods*, allowing identification of Tfn+ sCLSs and CCPs. Shown are **(A)** the mean A-647-Tfn fluorescence intensity grouped into CCP lifetime cohorts; error bars reflect cell-to-cell variation and dotted lines indicated the disappearance of clathrin from the TIRF field and **(B)** representative CCP trajectories depicting micrographs obtained by TIRF-M centered on the detected object and the quantification of the fluorescence intensity of eGFP-CLC and A-647-Tfn. **(C)** Shown is a histogram depicting the frequency of Tfn+ CCPs of indicated lifetimes.

**Supplemental Figure 10. Full-size representative TIRF images of RPE eGFP-LCa cells transfected with mCherry-Synaptojanin 1.** Shown in **Figure 8A** are TIRF-M images of RPE cells stably expressing eGFP-LCa and transfected with mCherry-Synaptojanin 1 (mCh-Sjn1, 170 kDa isoform). Shown here are the full-sized images of the representative TIRF-M images shown in **Figure 8A**, as well as the corresponding image frames obtained by widefield epifluorescence microscopy, scale, 20  $\mu$ m.

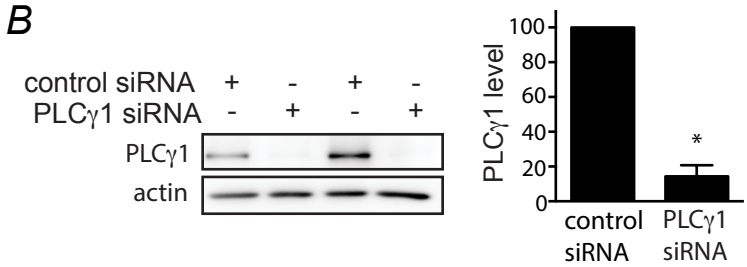
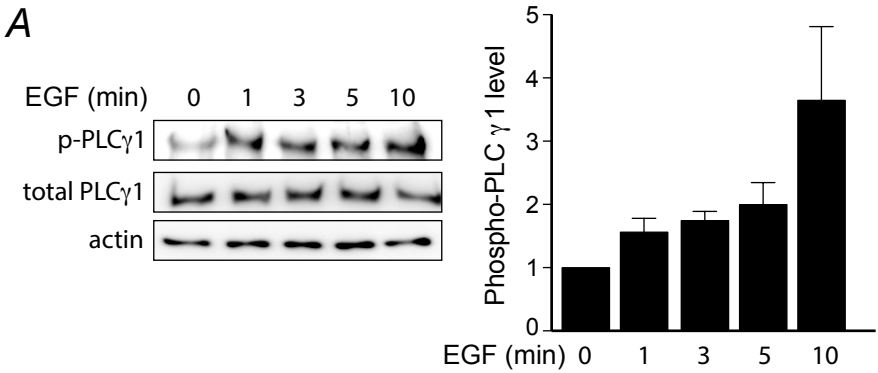
**Supplemental Figure 11. Endogenous synaptojanin 1 is depleted from CCPs upon EGF stimulation in a cytosolic Ca<sup>2+</sup>-dependent manner.** RPE cells stably expressing clathrin light chain fused to Tag-RFP-T (RFP-clathrin) were treated with 10  $\mu$ M BAPTA-AM for 15 min, 1  $\mu$ M Bisindolylmaleimide I -hydrochloride (BIM) for 30 min or left untreated (control), followed in some samples by stimulation with 5 ng/mL EGF, as indicated, then by immediate fixation and staining with anti-synaptojanin 1 (Sjn1) antibodies. **(A)** Shown are representative fluorescence micrographs obtained by TIRF-M, scale 10  $\mu$ m. Circles indicate CCPs positive for endogenous Sjn1, determined manually. **(B)** TIRF-M images were subjected to automated detection of CCPs, followed by quantification of mean Sjn1 fluorescence intensity therein. Shown in are median (bar) and 25th/75th percentiles (boxes) of Sjn1 fluorescence intensity within CCPs in each condition. The number of CCPs analyzed and cells, respectively, for each condition are as follows: basal, control (no drug): 20547, 68; basal, BAPTA-AM: 9839, 31; basal, BIM: 8843, 31; EGF, control (no drug): 19812, 65, EGF, BAPTA-AM: 7009, 31; EGF, BIM: 7817, 30; from 3 independent experiments. \*,  $p < 0.05$ , relative to the control, basal (non-EGF-stimulated) condition.

**Supplemental Figure 12. Perturbation of intracellular Ca<sup>2+</sup> impairs EGF-stimulated Akt phosphorylation.** RPE cells were treated with the cytosolic Ca<sup>2+</sup> chelator BAPTA-AM and then stimulated with 5 ng/mL EGF for 5 min. Shown are representative immunoblots for the indicated antibodies. BAPTA-AM treatment impairs EGF-stimulated Akt phosphorylation, but not that of Erk.

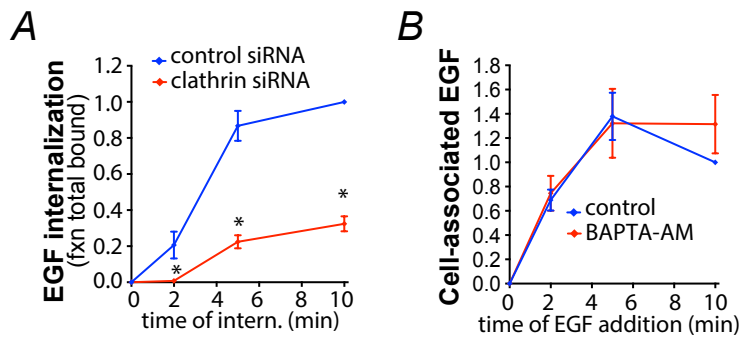
**Supplemental Figure 13. Model of regulation of CCPs harboring EGFR by PLC $\gamma$ 1-derived Ca<sup>2+</sup> signals and PKC.** Shown is a model showing the activation of PLC $\gamma$ 1 by EGFR, following by hydrolysis of PIP<sub>2</sub>, leading to generation of the secondary signaling intermediates inositol

trisphosphate (IP3) and diacylglycerol (DAG). IP3 agonism of the IP3 Receptor leads to an increase in cytosolic  $\text{Ca}^{2+}$ , which leads to an activation of conventional PKCs. This intracellular  $\text{Ca}^{2+}$  and PKC selectively control the initiation and size of clathrin-coated pits harboring EGFR, and thus the clathrin-dependent endocytosis and signaling of EGFR. Notably, EGF-stimulated  $\text{Ca}^{2+}$  signals are not required for the internalization of other clathrin cargo proteins such as TfR.

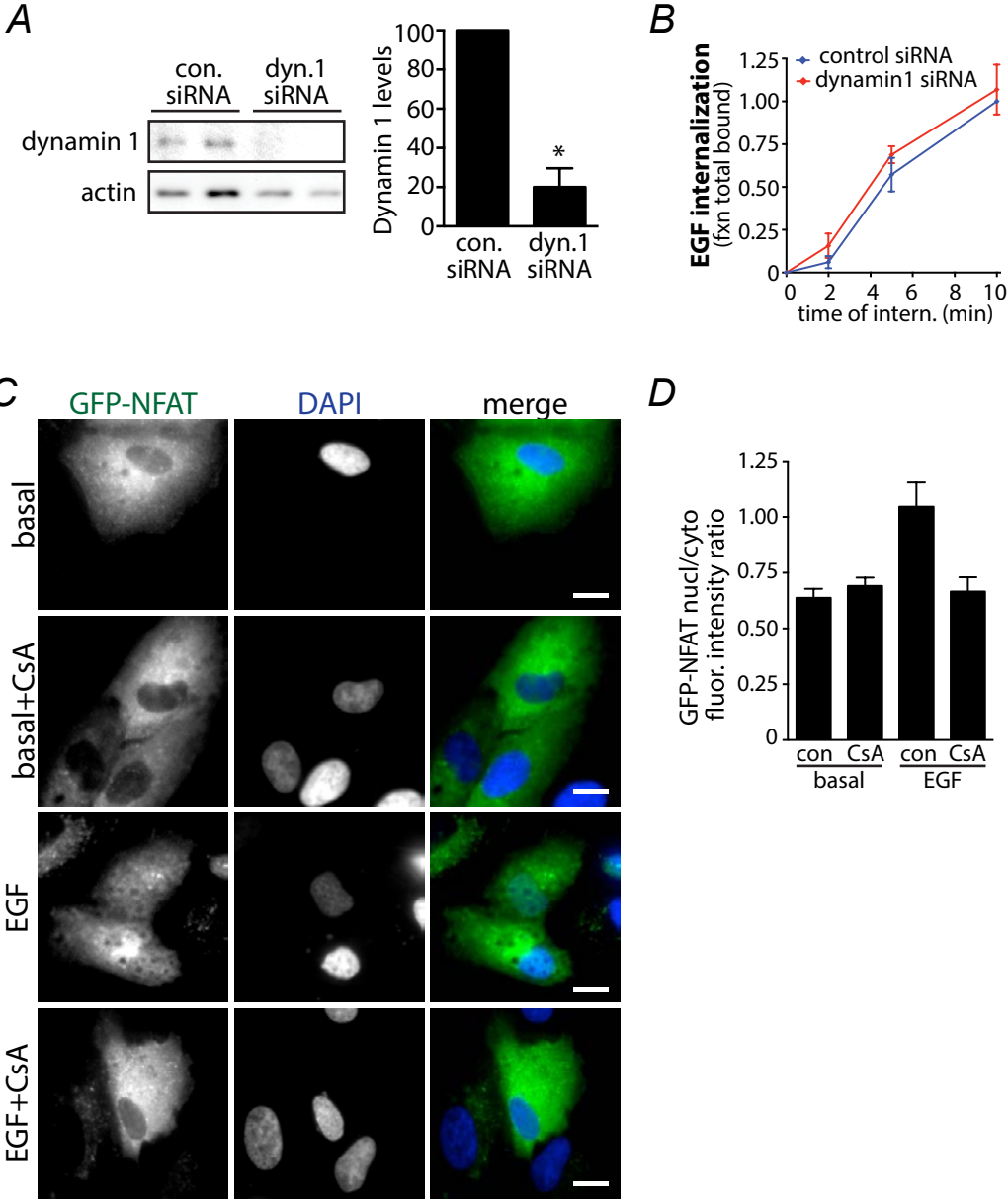
# Supplemental Figure 1



# Supplemental Figure 2

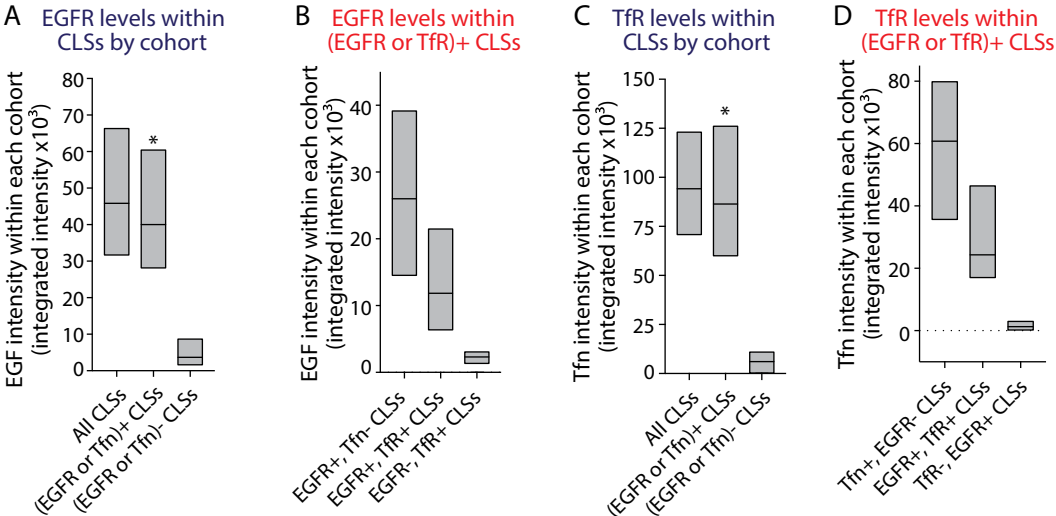


# Supplemental Figure 3

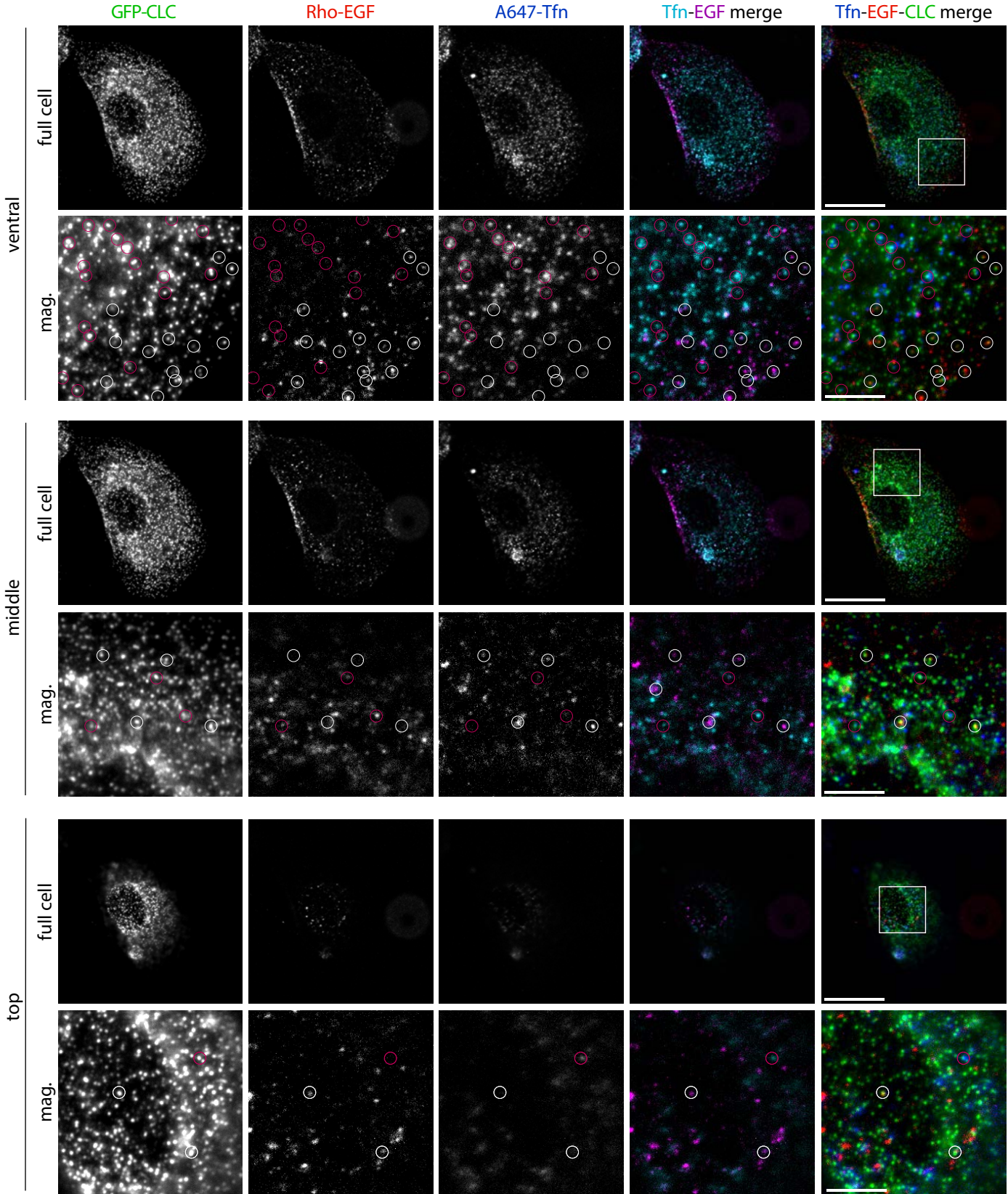




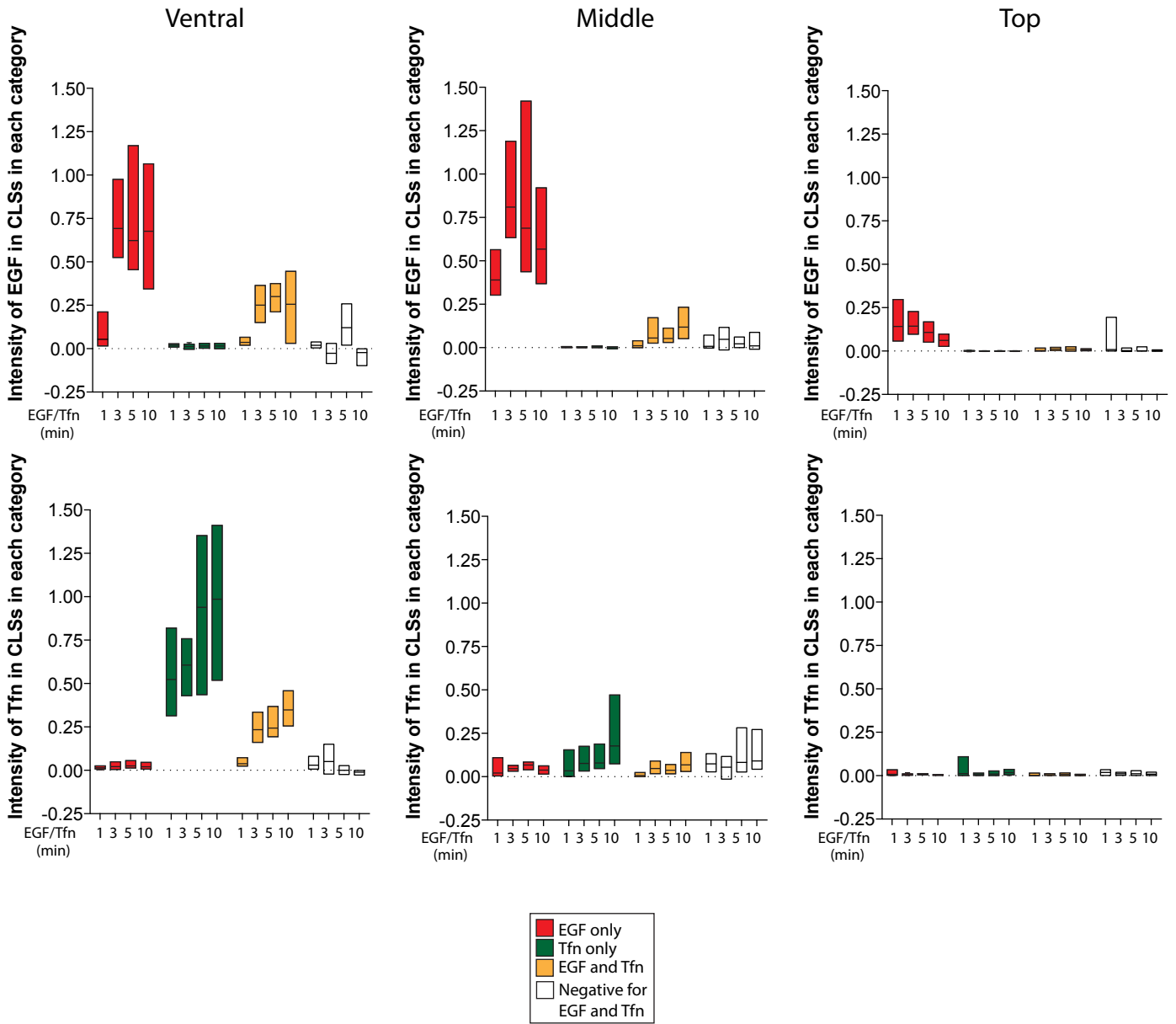
# Supplemental Figure 4



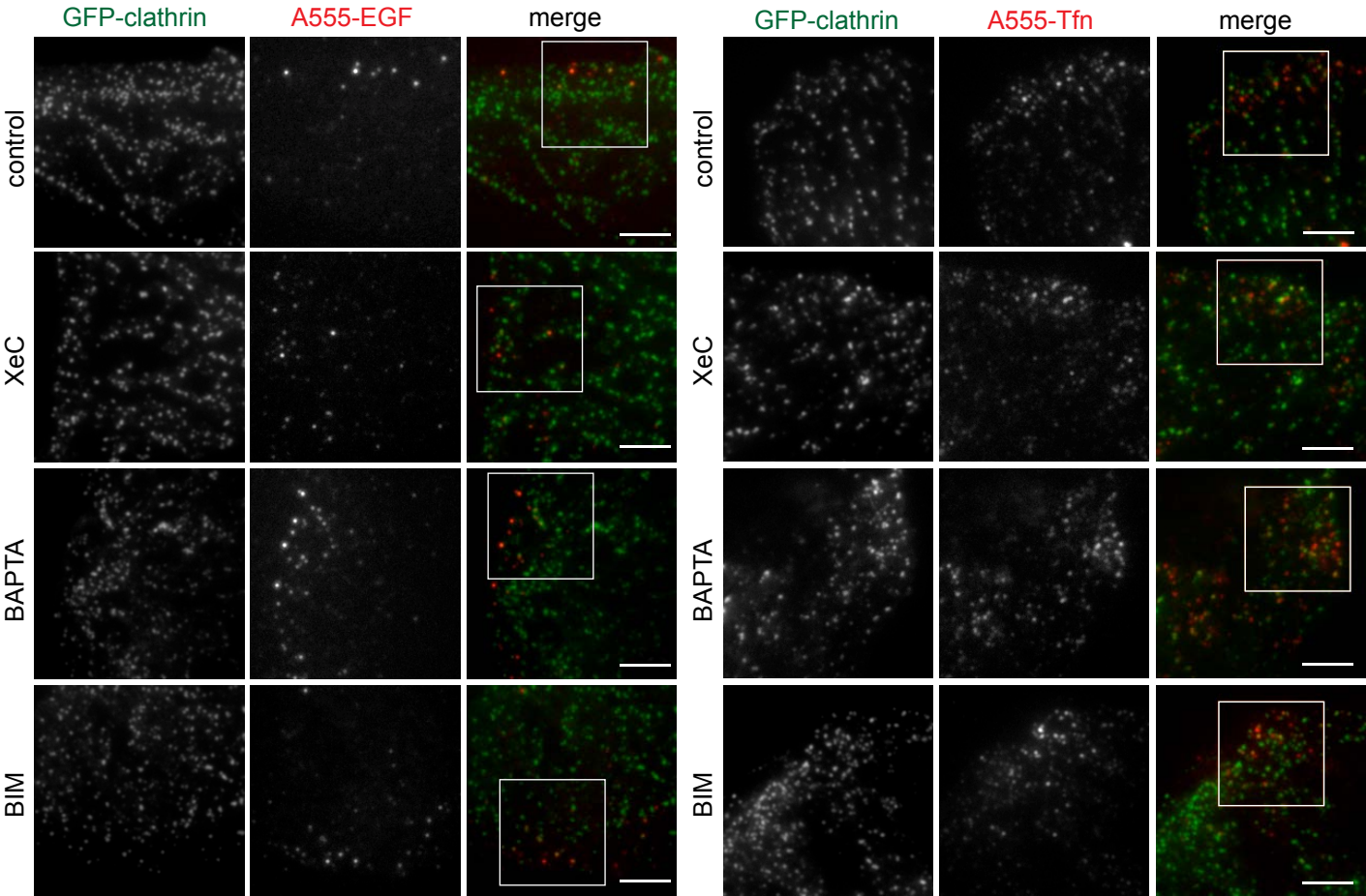
# Supplemental Figure 5



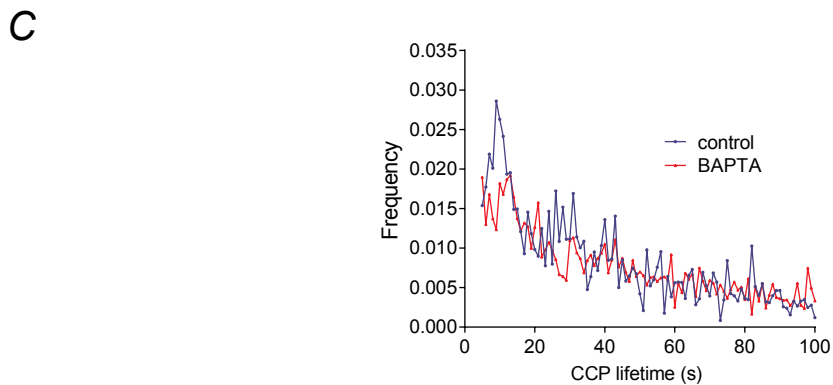
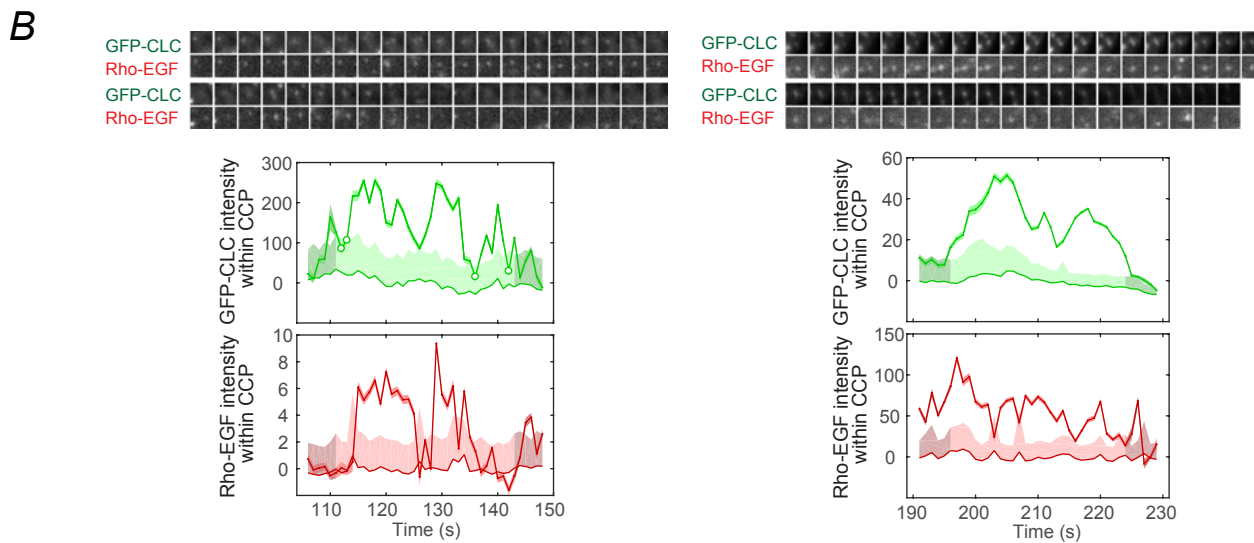
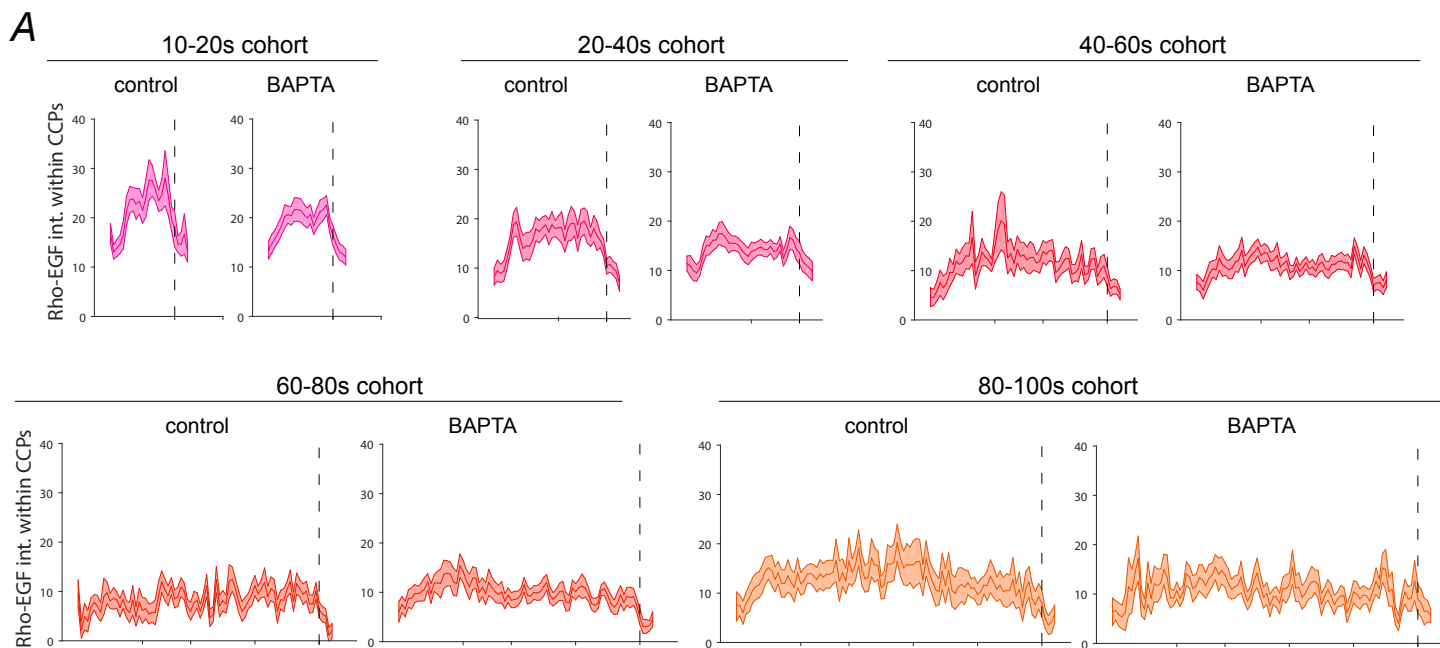
# Supplemental Figure 6



# Supplemental Figure 7

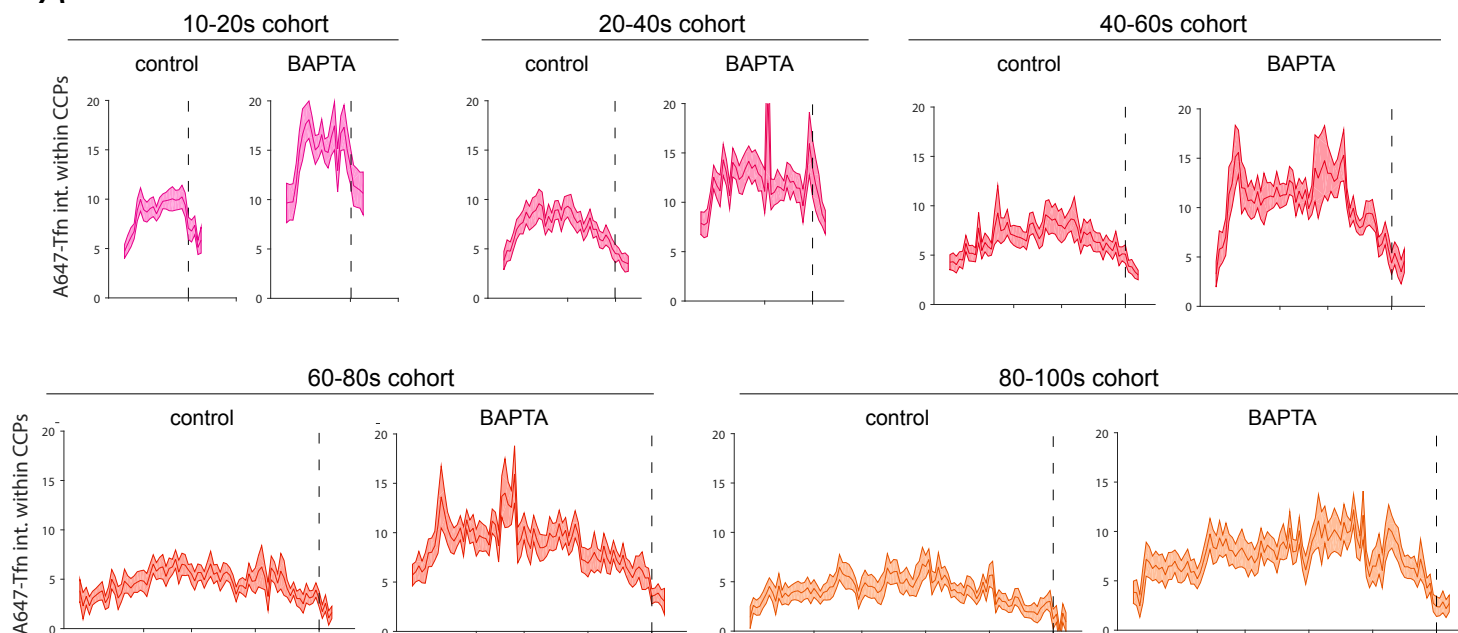


# Supplemental Figure 8

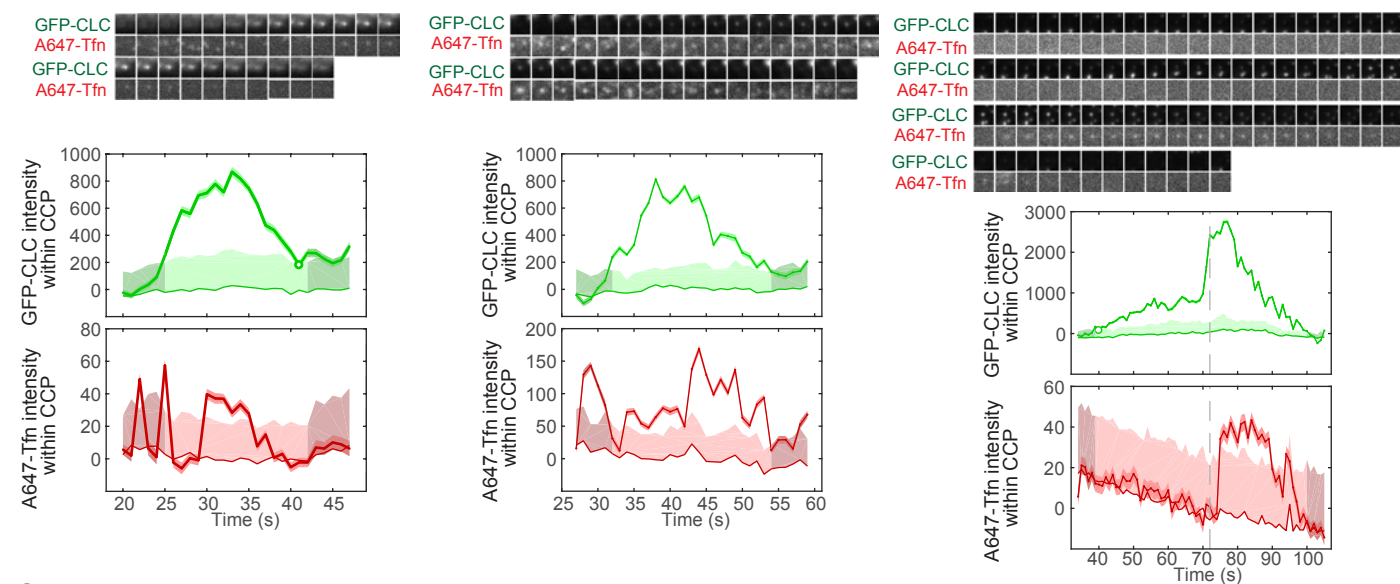


# Supplemental Figure 9

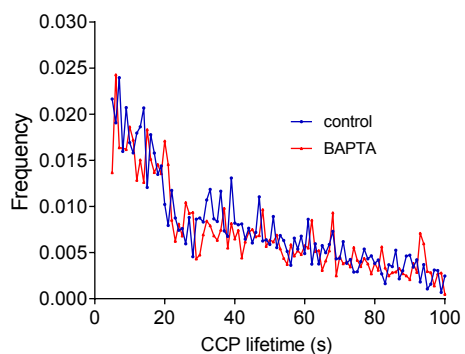
**A**



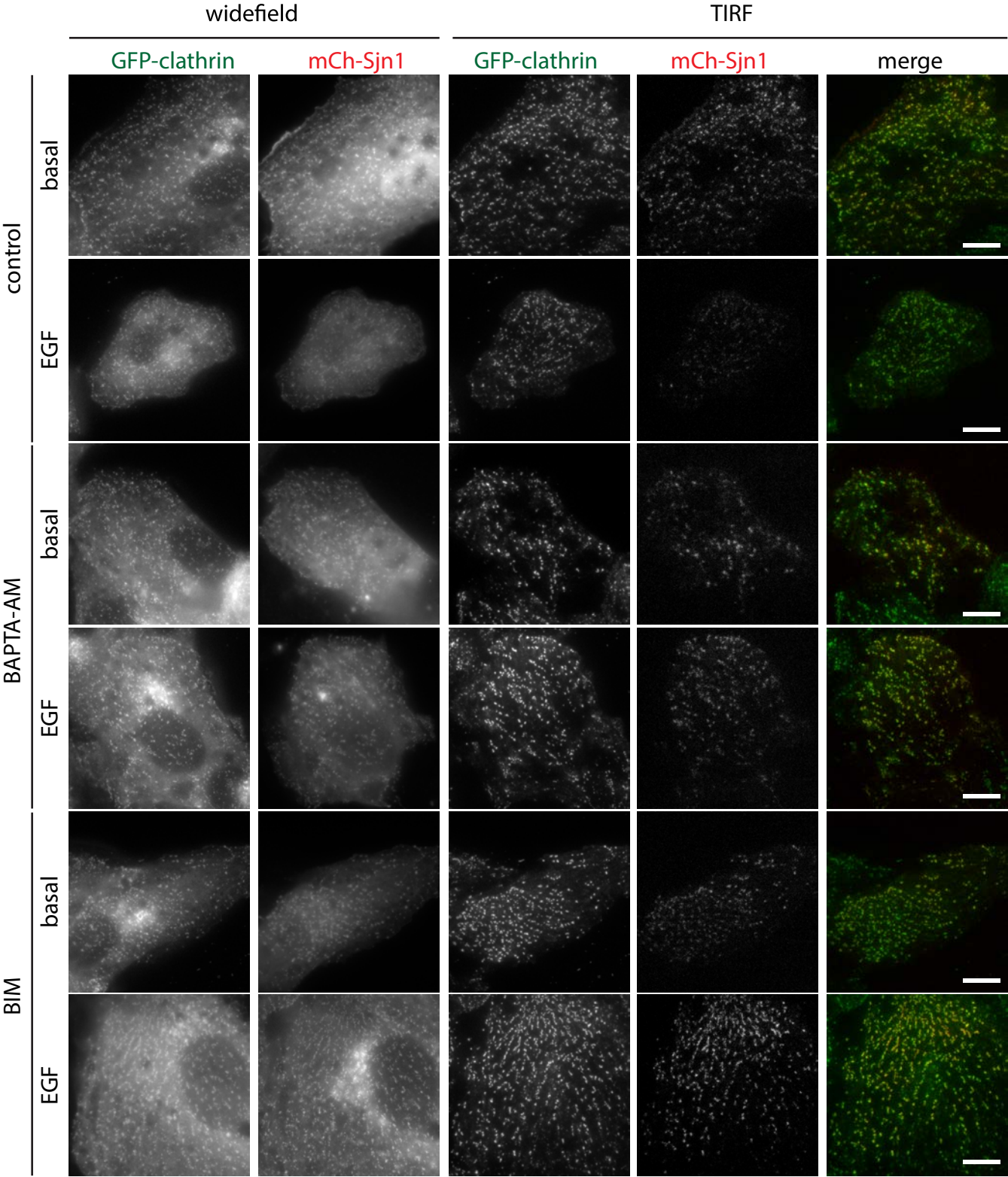
**B**



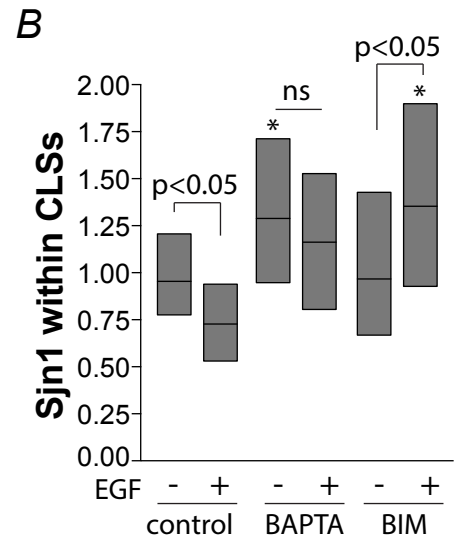
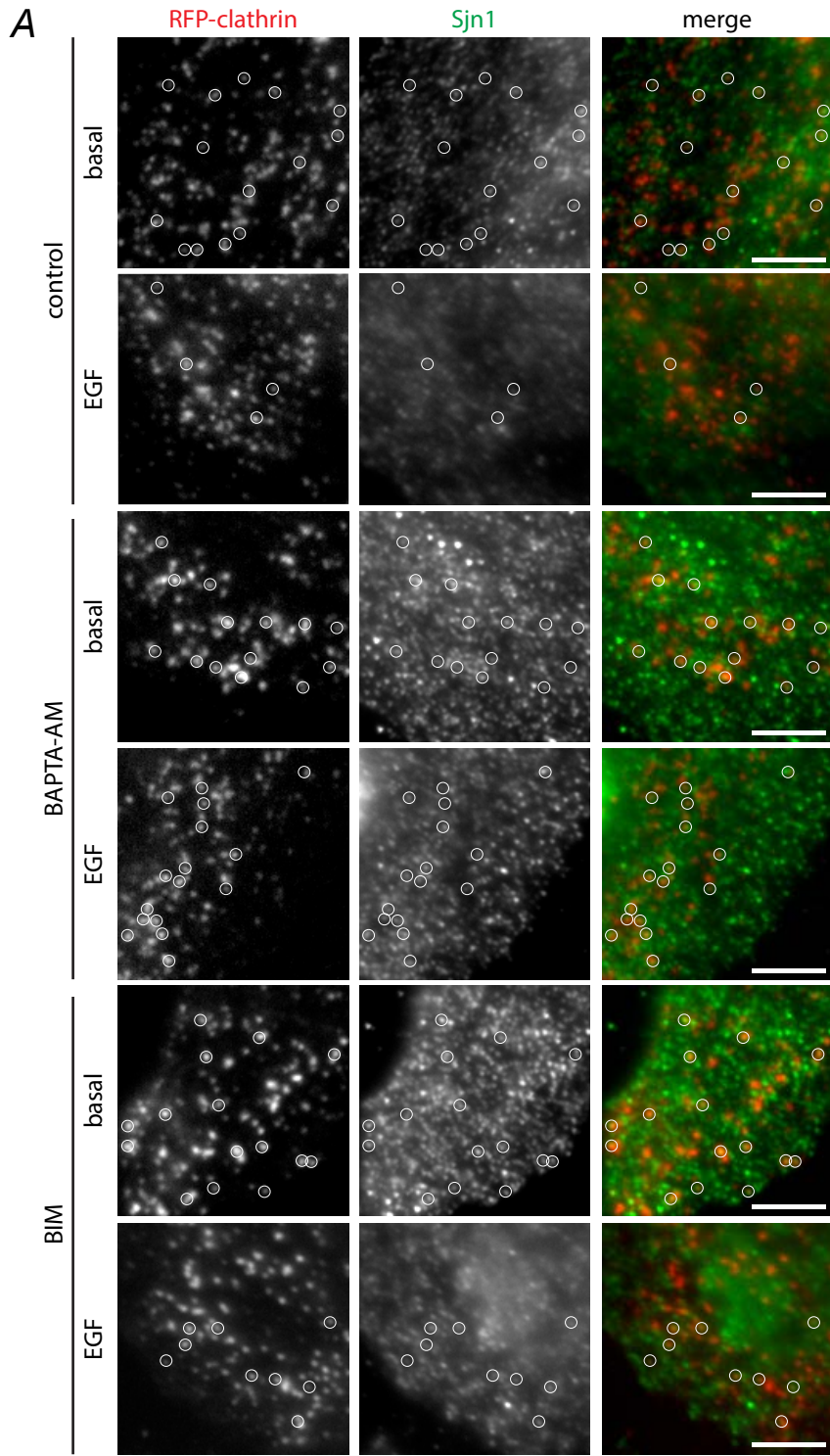
**C**



# Supplemental Figure 10

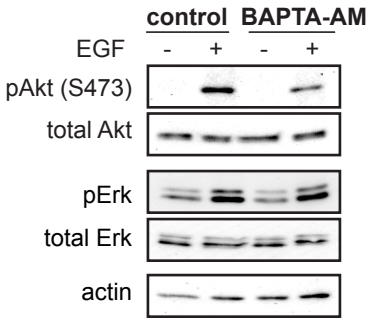


# Supplemental Figure 11





# Supplemental Figure 12



# Supplemental Figure 13

